

LAB-ON-A-CHIP TISSUE ENGINEERED 3D CANCER MODEL FOR *IN-VITRO* ANTI-CANCER DRUG SCREENING

*A Thesis Submitted in Partial Fulfillment of the Requirements
for the degree of*

**BACHELOR OF TECHNOLOGY
IN
BIOTECHNOLOGY**

By

RUKSAR SULTANA

110BT0621

Under the guidance of
Prof. Indranil Banerjee



**Department of Biotechnology and Medical Engineering
National Institute of Technology
Rourkela - 769008, Orissa, India
May 2014**

National Institute of Technology Rourkela



DECLARATION

I do hereby declare that the Project Work entitled “**Lab-on-a-chip Tissue engineered 3D cancer model for in-vitro anticancer drug screening**”, submitted to the Department of Biotechnology and Medical Engineering, National Institute of Technology, Rourkela is a faithful record of bonafide and original research work carried out by me under the guidance and supervision of Dr. Indranil Banerjee, Asst. Professor, Department of Biotechnology and Medical Engineering, National Institute of Technology, Rourkela, Orissa.

Date:

Place:

Ruksar Sultana

ACKNOWLEDGMENT

I would like to extend my deep sense of gratitude and my sincere thanks to my supervisor **Dr. Indranil Banerjee** for his constant guidance and encouragement. I am very much obliged for his patient counsel, invaluable suggestions, thoughtful and constructive criticisms without which this work would have been very difficult.

I thank with profound honor to **Prof. Krishna Pramanik**, Head of the Dept. of Biotechnology and Medical Engineering for her intellectual support and guidance throughout my study period.

I am indebted to all faculty members of the Dept. of Biotechnology and Medical Engineering for their advice and cooperation during the course of my study. I wish to express my gratefulness to **Dr. Kunal Pal**, **Dr. Sirsendu Sekhar Ray**, **Dr. Supratam Giri** for their constant help and for allowing me to use their instruments and materials. I am also thankful to other departments for permitting access to use their instruments.

I take immense pleasure in thanking my seniors, **Mr. Senthil Guru**, **Mr. Tarun Aggarwal**, **Mr. Prerak Gupta** for their invaluable help and suggestions which made my work easier by many folds.

I am also extremely thankful to **TEQIP- II (Technical Education Quality Improvement Program)** for accepting my application for funds to my product oriented project.

Needless to mention the support of all those who made my stay at Rourkela an unforgettable and rewarding experience.

Last but not least the least, I would like to thank my family members for rendering me enormous moral support during the whole tenure of my stay in NIT Rourkela.

Ruksar Sultana

National Institute of Technology Rourkela

Department of Biotechnology and Medical Engineering



CERTIFICATE

This is to certify that the thesis entitled "**Lab-on-a-chip Tissue Engineered 3D Cancer Model for in-vitro Anti-cancer drug screening**" submitted by Ms. RUKSAR SULTANA in partial fulfillment of the requirements for the award of the degree of Bachelor of Technology in Biotechnology at the National Institute of Technology, Rourkela is an authentic work carried out by her under my supervision and guidance.

To the best of my knowledge, the matter embodied in the thesis has not been submitted to any other University/ Institute for the award of any Degree or Diploma.

Date:

Place:

Dr. Indranil Banerjee

Assistant Professor

Department of Biotechnology and Medical Engineering
National Institute of Technology Rourkela

TABLE OF CONTENTS

LIST OF ABBREVIATIONS	7
LIST OF FIGURES	8
ABSTRACT	9
Chapter 1 INTRODUCTION AND REVIEW OF LITERATURE	10
1.1 Introduction	11
1.2 Conventional tumor models	13
1.3 In vitro 3D tumor models	15
Chapter 2 OBJECTIVE AND WORK PLAN	17
2.1 Rationale of the work	18
2.1.1 Choice of Biomaterials for scaffold fabrication	18
2.1.2 3D Microtissue	19
2.1.3 Lab-on-a-chip Device	19
2.1.4 Anticancer drugs	20
2.2 Objectives	20
2.3 Work plan	21
2.4 Design of the proposed model	22
Chapter 3 SCAFFOLD FABRICATION AND CHARACTERIZATION	23
3.1 Materials	24
3.2 Cell Culture	24
3.3 Preparation of Lab-on-a-chip device and its testing	24
3.4 Scaffold Fabrication	24
3.5 Scaffold Characterization	25
3.5.1 Fourier Transform Infrared Spectroscopy	25
3.5.2 X-Ray Diffraction	25
3.5.3 Microstructure Analysis	25
3.5.4 Swelling Study	26

	3.5.5 Biodegradation kinetics	26
	3.5.6 Biocompatibility study	26
	3.6 Suitability of gelatin-chitosan scaffold as cancer tissue mimic	27
Chapter 4	RESULTS OF SCAFFOLD CHARACTERIZATION	29
Chapter 5	FABRICATION OF 3D CANCER MODEL AND EVALUATION OF LAB-ON-A-CHIP DEVICES	36
	5.1 Hanging Drop Technique	37
	5.2 Microtissue formation	37
	5.3 Microtissue monitoring, characterization and optimization of cell number	38
	5.4 Seeding Microtissue on the scaffold	38
	5.5 Drug Susceptibility	39
	5.6 Cryopreservation	39
Chapter 6	RESULTS AND DISCUSSION	42
	6.1 Optimization of cell number for Microtissue formation	43
	6.2 Microtissue compactness and area growth kinetics	44
	6.3 Viability Assay of Microtissue seeded scaffold	45
	6.4 Anticancer Drug Cytotoxicity study	46
	6.5 Cryopreservation Performance	47
Chapter 7	CONCLUSION	48
Chapter 8	FUTURE WORK	49
Chapter 9	REFERENCES	50

LIST OF ABBREVIATIONS

%T	Percent Transmittance
vol.%	volume percent
2D	Two dimensional
3D	Three dimensional
DMEM	Dulbecco's Modified Eagle Medium
MEM	Minimal Essential Medium
FBS	Fetal Bovine Serum
KBr	Potassium Bromide
kV	kilo Volt
EDTA	Ethylene diamine tetraacetic acid
MTT	3-(4,5-Dimethylthiazol-2-yl)-2,5-Diphenyltetrazolium Bromide
ECM	Extracellular Matrix
M	Molar
rpm	revolutions per minute
nm	nanometer
ug	microgram
ml	milli liters
ul	micro liters
h	Hour
sec	seconds
θ	Theta
μ l	micro litres
μ m	micro metre

LIST OF FIGURES

Fig. No.	Title	Page No.
1	Drug Discovery Pipeline	12
2	Overview of Drug Discovery process	13
3	2D Monolayer	15
4	3D Spheroid	15
5	Use of animals for research	15
6	Design of the Proposed Lab-on-a-chip 3D Cancer Model	22
7	FTIR Spectra of gelatin-chitosan scaffolds	30
8	XRD Pattern of gelatin-chitosan scaffolds	31
9	SEM of gelatin-chitosan scaffolds	32
10	Swelling Kinetics of gelatin-chitosan scaffolds	32
11	Biodegradation Kinetics of gelatin-chitosan scaffolds	33
12	Biocompatibility of gelatin-chitosan scaffolds with HaCaT cells	34
13	SEM of HaCaT cells seeded on GC 21 scaffold 34	34
14	SEM of HeLa cells in 2D	34
15	SEM of HeLa cells seeded on GC 21 scaffold	34
16	Percentage cell death in response to varying doses of 5-FU and Cisplatin	35
17	Schematics of Cell aggregation, compactness and microtissue formation	37
18	Hanging Drop Culture	38
19	Phase Contrast Images of Microtissue at different cell density per drop	43
20	Approximately 32 hanging drops deposited & grown under a 15cm lid dish	43
21	Phase Contrast Images & Compactness profile of microtissue at day 4,5, 6	44
22	Area growth profile of microtissue from day 4, 5, 6	45
23	Cell Proliferation index of microtissue seeded scaffold construct compared to control system	45
24	Percentage cell death of microtissue seeded scaffold construct compared to theoretical predictions and control system	46
25	MTT Assay of cryopreserved microtissue seeded scaffold construct compared to control system which was not cryopreserved	47

Abstract

Development of in-vitro 3D cellular disease models is emerging at a fast pace. 2D culture systems are limited due to minimal cell-cell interactions and poor stromal intervention. Cells in 2D monolayer receive uniform oxygenation and nutrition in contrast to hypoxic conditions of in-vivo tumors. Hence, there is a need to develop 3D models which are more physiologically relevant than 2D models & improves the prediction of drug candidates. 3D models possess more realistic multicellular complexity (cell-cell, cell-matrix interactions) and mimics in-vitro microenvironment more closely. Present study delineates the development of a novel in-vitro 3D cancer model by incorporating cancer aggregates into porous scaffolds. This serves as a portable lab-on-a-chip platform for screening antitumor chemotherapeutic agents, For this purpose, gelatin–chitosan scaffolds were prepared by freeze-drying method, crosslinked using glutaraldehyde and investigated for their physical & functional characteristics such as micro architecture (SEM), FTIR, XRD, swelling property, degradation kinetics (using lysozyme) and biocompatibility. Microtissue comprising cervical cancer cells (HeLa) was prepared by suspending cancer cells in a hanging drop of culture medium followed by gravity enforced self assembly of cells into a solid mass. This cancer aggregate was embedded into the prepared porous scaffolds and cultivated in standard culture conditions. Microtissue viability in the 3D microenvironment of polymeric scaffold was assessed by MTT assay. Cryopreservation performance of microtissue seeded scaffold construct was examined by cooling using liquid N₂. Resuscitation of the constructs by thawing after 2 days of cryopreservation showed that system retained 76% of cell viability and metabolic activity. The constructs were then used as a cancer tissue mimetic to compare the efficacy of two anticancer drugs namely Fluorouracil (5-FU) and Cisplatin. Not all cells of the microtissue are exposed to the same drug concentration due to poor drug diffusion through the biomimetic scaffold which resembles native ECM. As predicted, percentage cell death is less in case of our model compared to conventional monolayer culture. These results clearly imply that the proposed gelatin-chitosan scaffold based 3D cancer model closely mimics in-vivo tumor conditions and can be used as an in-vitro screening system for anticancer drug screening.

Keywords: 2D, 3D model; cancer; chitosan; cisplatin; cryopreservation; lab-on-a-chip; gelatin; fluorouracil; HeLa cells; microtissue; scaffold

Chapter 1

**INTRODUCTION
AND
REVIEW OF LITERATURE**

1.1 Introduction

Cancer refers to abnormal growth of cells without control, ultimately evolving into a population that can invade other tissues by metastasis. It is one of the most serious diseases with millions of people who have cancer or have died because of its devastating effects. There are more than hundred different types of cancer. It is one of the most challenging disease of all - not only in terms of clinical barriers to its sufferers, but also to pharmaceutical companies and manufacturers who attempt to discover promising anticancer drugs.

Discovery and development of anticancer agents is the central focus of many pharmaceutical companies and other organizations, like the National Cancer Institute (NCI) [1]. Despite numerous efforts, successful development of cancer therapy is hindered by insufficient understanding of tumorigenesis. Anticancer drug development efforts focus on cytotoxic compounds that cause tumor termination. Recent spurt in the understanding of cancer pharmacology has facilitated the development of target-based drugs that are designed to selectively inhibit molecular markers involved in cancer growth and metastasis.

Once potential cytotoxic compounds are obtained by chemical synthesis or extraction from natural sources, the subsequent stages involved in drug development process are as follows:

1. **Preliminary in-vitro screening:** In-vitro cell culture models are used to evaluate anti-tumorigenic activity of new drug candidates. Approximately 10000 drugs are tested in in-vitro models on a yearly basis to investigate the extent and specificity of anti cancerous activity.
2. **Pre-clinical in-vivo testing:** Evaluation of drug toxicity and efficacy in animals.
3. **Clinical Development:** Drug toxicity is tested in human volunteers to identify maximum tolerated dose in phase I clinical trials. To quantify efficacy and to confirm drug dosage, phase II studies are conducted in patients of selected tumor type followed by massive phase III studies.

This entire process of drug discovery and development is innately time and resource

consuming with very low success rates. Out of 10,000 drugs screened, often only 100 are tested in pre-clinical research, 5-10 enter clinical trials and finally, only 1 or 2 compounds are eventually approved by NDA as marketed drug for treatment. The average time starting from a new compound synthesis to obtain market approval is approximately 9 to 12 years with average costs ranging from 0.5 to 2 billion US\$ depending on the disease.

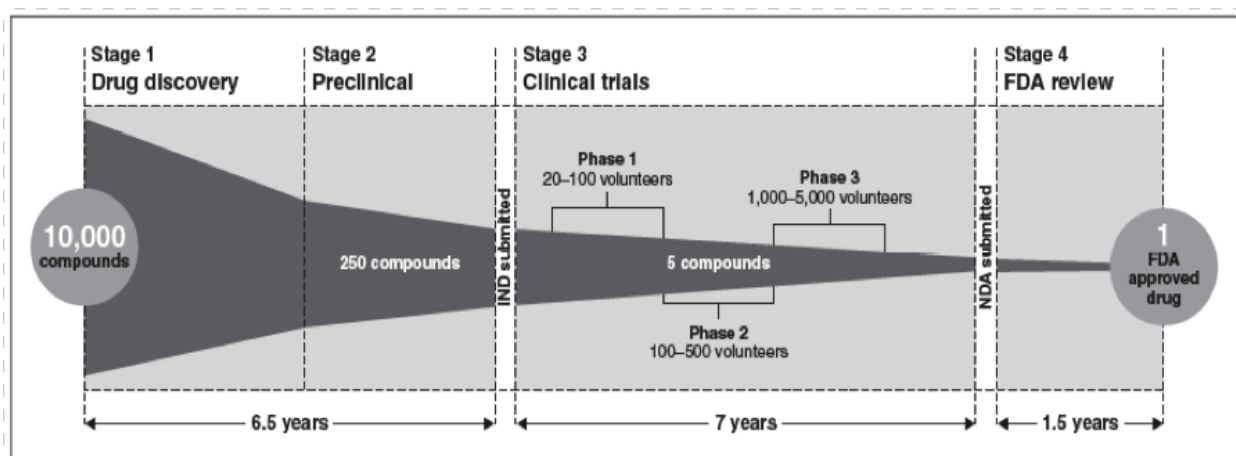


Fig.1 Drug Discover Pipeline. (PhRMA - The Pharmaceutical Research and Manufacturers of America, IND - Investigational New Drug)

Preclinical and clinical drug development has predominantly relied on animal systems. The time and costs of drug development significantly increases during pre-clinical in-vivo testing using animals and further more in subsequent clinical trials, it is pivotal to identify promising drug leads accurately in the early stages of drug development [2]. Successful selection and development of the most active drug candidates requires reliable and robust in-vitro test systems. Novel approaches have been adopted for creating dependable in-vitro models that mimic in-vivo tumor behavior. Complex interaction between multiple cell types operating within the 3D tissue ECM microenvironment is highly critical for tissue development, homeostasis and tumor pathogenesis. Gene expression, invasive behavior of many human carcinomas are sensitive to 'solid factor signals' and behaves entirely different in the presence or absence of stroma. Existing in-vitro models include - 2D monolayer culture and 3D spheroid models.

3D Spheroids: Spheroids refer to in-vitro aggregate of cells established either from a single cell type or from a mixture of multiple cell types: tumor cells, immune cells, epithelial cells, fibroblast cells, mesenchymal stem cells (MSCs) and endothelial cells. These aggregates are more effective than 2D systems because like tumors, spheroids usually contain a mixed population of surface-exposed and deeply buried cells, proliferating and non proliferating cells, well-oxygenated and hypoxic cells [3]. Though it maximizes cell-cell interactions, it inherently lacks stromal intervention. The average time required for a tumor spheroid to advance from an aggregate of few cells to an enlarged structure with viability and proliferative gradients ranges from 1 to 2 weeks. It is highly challenging to obtain spheroids of uniform size in a reproducible manner.

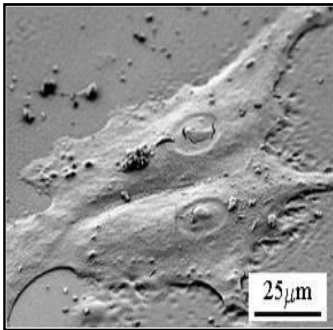


Fig.3 2D Monolayer

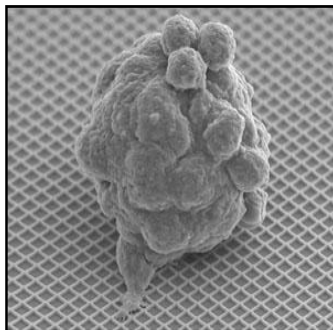


Fig.4 3D Spheroid



Fig.5 Use of animals for research

An apparent solution to the above models is to use in-vivo animal models.

Animal Models: Though scientific values and ethics of using animals for research are continuously being questioned, it is estimated that millions of animals are still widely used in variety of different research projects every year. Though, in vivo models address some of the limitations of in-vitro systems, ethical concerns, long experimental duration and non-human biology represents significant disadvantages. Besides, drugs and procedures that seem promising in animal models have often failed in early or later phases of clinical trials. Besides the cost of drug development increases substantially during pre-clinical in-vivo animal testing. Hence, we need to **Reduce, Replace** and **Refine** the use of animals. One of the elemental problems is low predictivity from currently employed preclinical research models. For economic and ethical

concerns, this necessitates the development of 3D cancer models which overcome the gap between traditional 2D monolayer and animal models.

1.3 In vitro 3D tumor models:

It is highly essential to identify poor drug candidates in early stages of testing than later which would save both time and money. To optimize accurate selection of the most active drug molecules from the enormous and growing pool of compounds, test systems that closely simulate an *in vivo* solid tumor are highly essential.

Hence, we need to create more realistic *in-vitro* cell culture models which faithfully replicates *in-vivo* microenvironment. However, the realization of thick and viable disease equivalents *in vitro* is one of the major challenges in tissue engineering [4]. A biological tissue is not just a combination of cells within a bundle of inert macromolecules, but it is rather an intricate complex of cell and cell-synthesized matrix regulated by homeostatic equilibrium. Cells are regulated and controlled by the ECM composition and structure, which, in turn, are synthesized, assembled and remodeled by cells. Tissue dysfunction even when arisen from cellular components affects the extracellular space and vice versa [4]. Therefore, a reliable *in-vitro* 3D cancer model should reproduce the whole tissue, including the ECM assembly in order to faithfully and realistically mimic both the physiological and pathological status of *in-vivo* cancerous tissue.

In-vitro 3D cancer models mimicking biologically important parameters of *in-vivo* microenvironment such as cell–cell, cell–ECM interactions will be a valuable device to examine the therapeutic efficacy of anticancer drugs [5]. 3D models are increasingly been used to accurately reproduce characteristics and behavior of human cancerous tissues. Novel strategies are being employed for creating better reliable *in-vitro* models that better recapitulate *in-vivo* conditions for testing the anti tumorigenic efficacy of anticancer drugs. These models also have the potential to improve and to optimize drug delivery systems for effective chemotherapy.

The importance of *in-vitro* 3D tumor models has been widely recognized and their development

is emerging at a fast pace. Crystal S. Shin et al have adapted hydrogel template to culture spheroids in a hydrogel scaffold containing micro wells and subsequently transferred the spheroids to a microfluidic channel representing in-vivo dynamic fluid movement [5]. Hui-li Ma et al have demonstrated the capability of HeLa cell-derived spheroids to function as a screening tool for nanoparticle which act as delivery vehicles for chemotherapeutics [6]. They have reported three dimensional imaging of nanoparticle penetration into HeLa spheroids using HeLa cells grown in 2D culture as the control system. Moutushy Mitra et al have fabricated surface engineered, polymeric biodegradable microparticles to be used as a scaffold for 3D growth of Y79 cell line in order to evaluate the effect of anticancer drugs [7]. Qgyi He et al have tissue engineered a pancreatic cancer model using pancreatic cancer stem cells delivered from a well defined electrospun scaffold of poly(glycolide-co-trimethylene carbonate) and gelatin [8]. Agata Nyga et al have constructed a novel colorectal cancer model using HT29 cells embedded in collagen type I which is encapsulated in a non-dense collagen type I gel populated by a mixture of fibroblasts and endothelial cells [9]. Jayme L. Horning et al have developed a breast cancer model by cultivating MCF-7 cells on porous, biodegradable polymeric microparticles [10]. Chandraiah Godugu et al have reported a 3D culture system for formation of spheroids in Alginate™ scaffolds and subsequent cytotoxicity evaluation of anticancer drugs [11].

Chapter 2

OBJECTIVES AND WORK PLAN

2.1 Rationale of the work :

The present study was conducted to develop a viable lab-on-a-chip 3D cancer equivalent with high in-vivo like characteristics and better predictivity than 2D monolayer and 3D spheroid models. Spheroids are more physiologically relevant than 2D monolayer as they overcome the limitations of 2D systems by maximizing cell-cell interactions. However, they lack stromal intervention which provides tumor promoting microenvironment highly essential for tumor growth, invasion and metastasis. Hence, spheroid models alone fail to mimic in-vivo tumor microenvironment. As an improvement over existing cancer models, we have proposed a novel 3D cancer model by incorporating tumor like aggregates in a porous biomimetic scaffold. Cell-cell interactions within the aggregate and cell-matrix interactions between the scaffold and aggregate forms a complex network of biochemical and mechanical signals, which are critical for tumor physiology. We have tried to address the relevance and potential of this 3D cancer model in drug discovery and development, with a focus on screening anticancer drugs. Furthermore, we have also proposed to assess the cryopreservation feasibility of this model to investigate its ready-to-use application in evaluating drug efficacy and toxicity after resuscitation. This innovative simplified preclinical approach will offer faster reliable results with far greater in vitro predictive power.

2.1.1 Choice of Biomaterials for scaffold fabrication:

Scaffold acts as an artificial ECM and provides structural and biochemical support to cells until the cell produced ECM (collagen) takes over its function. This study demonstrates the use of porous 3D gelatin-chitosan scaffolds as a tissue culture model for supporting the growth of microtissue. Chitosan has gained a lot of attention as a promising biomaterial in tissue engineering due to its large-scale availability, low cost, biocompatibility and anti-microbial activity [12]. Chitosan backbone mimics glycosaminoglycans (GAGs) structure, a major component of the native ECM. Chitosan is blended with other polymers in order to improve its biological, mechanical and physiological property. To improve the biological activity of chitosan, gelatin (collagen mimic) is used since it (i) contains Arg–Gly–Asp (RGD)-like sequence which promotes cell adhesion and migration and (ii) forms a polyelectrolyte complex

[12]. Gelatin-chitosan scaffolds have been fabricated using crosslinkers such as glutaraldehyde, EDC-MES. Constructs formed upon embedding microtissue into these biomimetic scaffolds provides a reliable and cost-effective an vitro platform for evaluating the efficacy of anticancer drugs.

2.1.2 3D Microtissue:

Microtissue or microscale spheroids are relevant constructs for tissue engineering applications to evaluate toxicities of anticancer drugs.. Formed from cancer cells in hanging drops, microtissue mimics a tumor in vitro. Cytology and morphology of micro- or millimeter tumor microtissues bears a resemblance to in-vivo grown avascular tissue or natural human tumors before neovascularization with diffusional limitations. Three-dimensional tumor microtissues acquire resistance to apoptosis-inducing drugs that mimics chemoresistance of solid tumors. Furthermore, microtissues can be handled easily in a cost-effective manner and are a faithful replica of native cancerous tissue. 3D tumor microtissue bridges the gap between in-vitro 2D cell assay and in-vivo animal models and offer powerful reliable in-vitro test systems for investigating compound efficacy and toxicity.

2.1.3 Lab-on-a-chip device:

Lab-on-a-Chip (LOC) is a device which integrates various laboratory functions such as separation and analysis of components of a mixture on a single microchip. It uses small fluid volumes in the order of microliters to nanoliters. The main commercial application of LOCs is in biotechnology and medical fields, where it can be used as novel microsensing systems. This is a newer cell based approach which merges microfluidics and imaging tools with modern tissue engineering by integrating in vitro produced pieces of cancer tissue mimic on microfluidic chips. The chip holds an array of microwells each comprising cancer microtissue embedded in a biomimetic scaffold mimicking cancer microenvironment. This portable, easy-to-use chip miniaturizes testing system and enables rapid, reliable and cost-effective assessment of the antitumorigenic effect of any given chemotherapeutic compound.

2.1.4 Anticancer drugs:

Two most commonly used drugs: 5-Fluorouracil (5-FU) and Cisplatin were used in our analysis. Both these drugs are often used to treat various types of cancers.

5-Fluorouracil (5-FU): a conventional anticancer drug which has been used against various types of cancers for many years. It is principally a suicide inhibitor of thymidylate synthase (TS), a nucleoside required for DNA replication. Deoxyuridine monophosphate (dUMP) is methylated by Thymidylate synthase to form thymidine monophosphate (dTMP). dTMP deficiency caused upon administering 5-FU triggers apoptosis of rapidly dividing cancerous cells.

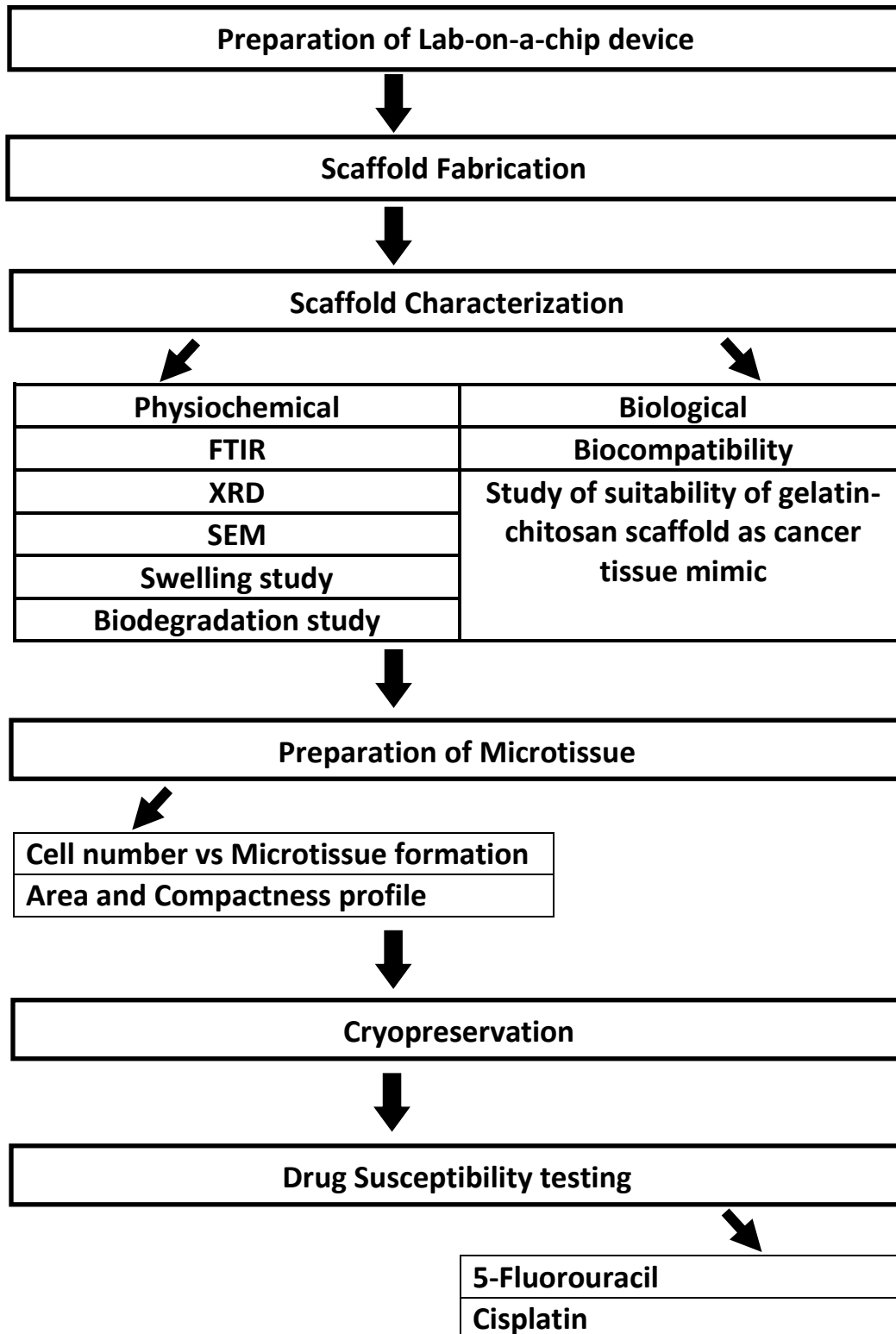
Cisplatin: is a conventional chemotherapy drug particularly effective against testicular cancer. It binds to DNA and causes it to crosslink, subsequently interferes with the process of cell division by mitosis. DNA repair mechanism is activated by the damaged DNA, which in turn triggers apoptosis when repair seems impossible.

2.2 Objective:

To develop an *in-vitro* 3D cancer model that replicates *in-vivo* tumor behavior to be used as a screening tool to evaluate chemotherapeutic efficacy of anticancer drugs.

1. Preparation of Lab-on-a Chip platform
2. Fabrication of suitable tissue mimicking 3D scaffold
3. Preparation of cancer microtissue
4. Preparation of corresponding cancer tissue construct on lab-on-a-chip platform
5. Evaluation of the model as anticancer drug screening system.

2.3 Work plan:



2.4 Design of the Proposed Model:

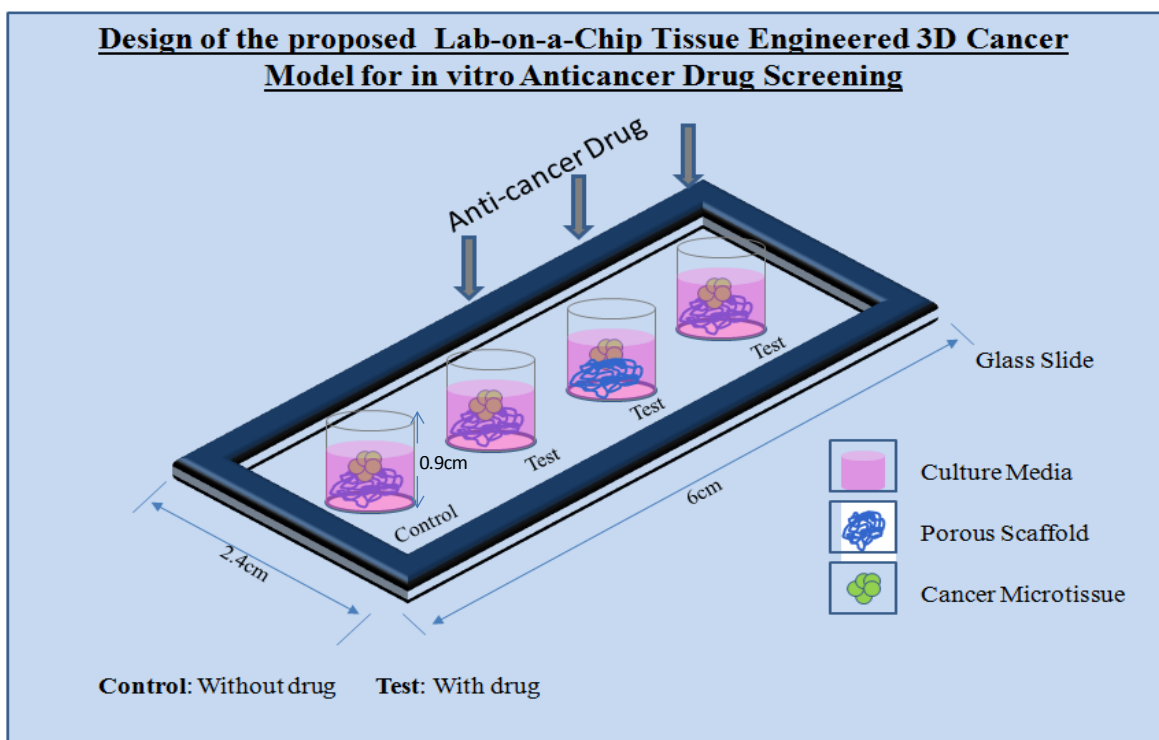


Fig.6 Design of the Proposed Lab-on-a-chip 3D Cancer Model

Chapter 3

SCAFFOLD FABRICATION AND CHARACTERIZATION

3.1 Materials

Gelatin (from bovine skin) and chitosan were procured from SIGMA ALDRICH. Glutaraldehyde (25% aqueous solution) was purchased from LOBAL CHEMIE (Laboratory Reagents & Fine Chemicals). For cell culture, DMEM, MEM, Dulbecco's Phosphate Buffer Saline (DPBS), Trypsin-EDTA solution, FBS, antibiotic-antimycotic solution, and MTT assay kit were purchased from Himedia, Mumbai, India. For cell lysis IP lysis buffer Pierce was procured from Thermo scientific. Millipore water was used throughout the study.

3.2 Cell culture

HeLa (cervical cancer) cell line were cultured in flasks coated with gelatin and maintained in complete medium consisting of Minimal Essential Media (MEM) supplemented with 10% Fetal Bovine Serum (FBS) and 1% antibiotic-antimycotic cocktail in a humidified (95%), CO₂ incubator (5%) at 37°C. When the cells reached about 70% confluence, they were harvested by dissociating cells using 0.25% Trypsin-EDTA solution, followed by centrifugation of the dissociated cells at 1000 rpm for 10 minutes, and re-suspended in complete media. Cell density was estimated using a hemocytometer. HaCaT cell line was maintained in Dulbecco's Minimal Essential Media (DMEM) following the same protocol.

3.3 Preparation of Lab-on-a-chip device

Polypropylene sheet was cut into chips of dimension 6 cm x 2.4 cm. The chips were thoroughly washed in Triton-X solution and then immersed in 70% ethanol solution for 10 minutes. They were then dried and micro wells were attached using poly-dimethylsiloxane (PDMS). The assembly was then baked at 65°C in a hot air oven for 1 hour. The PDMS gets spontaneously adhered to the plastic chip thus maintaining a tight sealing. In this way, microwell arrays were fabricated onto the chips.

3.4 Scaffold Fabrication:

2% gelatin solution was prepared by mixing gelatin in Millipore water on a magnetic stirrer at 50 °C for 30 min. 2% Chitosan solution was prepared by dissolving chitosan in 1 vol.% acetic acid at room temperature. Three different compositions of mixture were prepared - (Gelatin:

Chitosan 1:1, 1:2, 2:1). The solutions were thoroughly mixed to have required weight ratio of gelatin to chitosan by stirring at 50 °C for 30 min until a homogeneous mixture was obtained. 0.025% glutaraldehyde was added for cross linking and stirred for another 15 minutes. Thereafter, 250ul of each solution was immediately transferred to each microwell of lab-on-a-chip device avoiding gelation prior to transferring. Gelatin-chitosan scaffolds were fabricated by freezing overnight at -20°C followed by lyophilization for 36 h to obtain dry, porous scaffolds. The scaffolds are referred to from now on as GC21, GC11, GC12 for gelatin/chitosan ratio of 2:1, 1:1 and 1:2, respectively (G gelatin, C chitosan).

3.5 Scaffold Characterization

3.5.1 Fourier Transform Infrared Spectroscopy:

The composite scaffold samples were ground into fine powder by freezing in liquid N₂ for 30 minutes. FTIR imaging of the samples was carried out by using Shimadzu/ IR Prestige 21. 1mg of each sample was mixed with IR-grade KBr so as to maintain 2% sample to KBr ratio. KBr pellet of the samples were prepared using KBr Press till 0-10 tons. Background scanning was first conducted using blank KBr pellet and subtracted from the sample readings. Then the samples were scanned in the region 400 cm⁻¹ to 4000 cm⁻¹ and a plot of wavenumber (cm⁻¹) vs %T is prepared.

3.5.2 X-Ray Diffraction:

Sample was carefully placed in sample holder and subjected to X-ray diffraction in 2θ ranging from 5° to 40° with a step size of 0.05° and scanning rate 7° per minute.

3.5.3 Microstructure analysis:

Surface morphology of the scaffolds was examined by field emission scanning electron microscope (NOVA NANOSEM). The lyophilized scaffolds were cut with a razor blade to expose the inner surfaces and mounted on specimen stubs containing two-sided carbon tape. The samples were coated with gold particles in a sputter coater, FESEM images of the scaffolds were

acquired at an operating voltage of 20 kV. Average pore size of the scaffolds was measured by determining the average of random 25 pores using ImageJ software.

3.5.4 Swelling Study

Swelling ability of the scaffolds was studied by placing in phosphate buffered saline (PBS), pH 7.4 at 37°C. The initial dry weight of the scaffolds were noted as W_1 . The wet weight (W_s) of the scaffold was noted by weighing it while excess water was blotted out with absorbent paper. Wet weight was recorded at predetermined time points and noted as W_2 . Swelling ratio was calculated using the following equation:

$$\text{Swelling ratio (\%)} = (W_2 - W_1) / W_1 \times 100$$

where W_2 is the wet weight of the scaffolds and W_1 is the initial dry weight of the scaffolds.

3.5.5 Biodegradation Kinetics

Biodegradation of the scaffolds was studied in-vitro by incubating the scaffolds in PBS (pH 7.4) at 37°C containing 1 ug/ml hen egg lysozyme. The control system included scaffolds incubated in PBS without enzyme. At predetermined time-periods, the scaffolds were removed from the PBS solution containing enzyme, washed with Millipore water and lyophilized for 48 h. The extent of in vitro biodegradation was expressed as a percentage of the remaining weight of the dry scaffolds after enzyme treatment. Percentage biodegradation was determined using the equation:

$$\text{Biodegradation (\%)} = (W_d / W_0) \times 100$$

where W_0 is the initial dry weight of the scaffold and W_d is the dry weight of the degraded scaffold recorded at predetermined time points.

3.5.6 Biocompatibility study:

i) Pre-culture Scaffold Preparation:

Scaffolds were neutralized by immersing in 0.1M Glycine for 1 h to remove acetic acid, followed by washing three times with PBS (pH 7.4). Then the scaffolds were sterilized by exposure to UV light for 1 h. Scaffolds were further sterilized with 70% (v/v) ethyl alcohol for 1 h followed by washing three times with PBS to remove ethanol. Scaffolds were then equilibrated in complete medium for 1 h before cell culture.

ii) Cell seeding and culture on scaffolds:

Media was removed and HaCaT cells were seeded on the scaffold at required cell density. The seeded constructs were incubated in a humidified incubator for cell growth and proliferation. MTT assay was used to access biocompatibility of the scaffolds.

MTT Assay:

MTT assay is used for determining cell viability and cell proliferation and/or effect of cytotoxic agent. It is based on the quantitative measurement of extracellular reduction of yellow colored water soluble Tetrazolium dye 3-[4, 5-dimethylthiazol-2-yl]-2, 5-diphenyl tetrazolium bromide (MTT) to insoluble formazon crystals by metabolically active cells. The reduction is mediated by mitochondrial enzyme lactate dehydrogenase. When dissolved in a solubilization solution such as dimethylsuphoxide (DMSO), these formazon crystals exhibit purple color. The intensity of this color is proportional to the number of viable cells and can be measured spectrophotometrically at 570nm. MTT Reagent is added to a final concentration of 10% of the total volume.

iii) SEM of cell seeded scaffold:

Scanning electron micrograph of cell seeded scaffold was taken after fixing the cells. Fixing was done by immersing the cell seeded scaffolds in SEM buffer containing 2.5% glutaraldehyde for 2h. Scaffolds were critically dried using graded ethanol treatment (30%, 50%, 70%, 90%, 95%, 100% ethanol) each of 15 minutes duration.

Statistical analysis: All experiments were performed in triplicates for each sample and data is expressed as mean \pm standard deviation (SD) for n=3.

3.6 Suitability of gelatin-chitosan scaffold as cancer tissue mimic

Scaffolds were neutralized and sterilized using the same afore-mentioned protocol. HeLA cells were seeded on the scaffold at a cell density (5×10^4). The seeded constructs were incubated in a

humidified incubator for 2 days to allow cell growth and proliferation within the porous scaffold. Stock solutions (1mg/ml) of two drugs - Fluorouracil (5-FU) and Cisplatin was prepared in PBS.

3.6.1 Drug Treatment

The cell seeded scaffold constructs were analyzed for their chemotherapeutic sensitivity to 5-FU and Cisplatin at two different concentrations (10ug/ml, 50ug/ml) for each drug. Effect of these cytotoxic agents on cell viability and proliferation within the scaffold was accessed by MTT assay. The control system included HeLa cells directly cultured in the microwell at the same cell density as seeded on the scaffold.

Chapter 4

RESULTS OF SCAFFOLD CHARACTERIZATION

4.1 FTIR analysis:

The inter-molecular interaction can be determined by FTIR when two polymers are blended together to form a scaffold. In case of GC blends, FTIR analysis was conducted by identifying absorption bands associated with the vibrations of functional groups present in the macromolecules. Exactly similar FT-IR spectra was obtained from the three blends: GC 21, GC 11, GC 12. Hence, we can state that varying the ratio of gelatin and chitosan has no effect on the molecular structure of GC scaffolds.

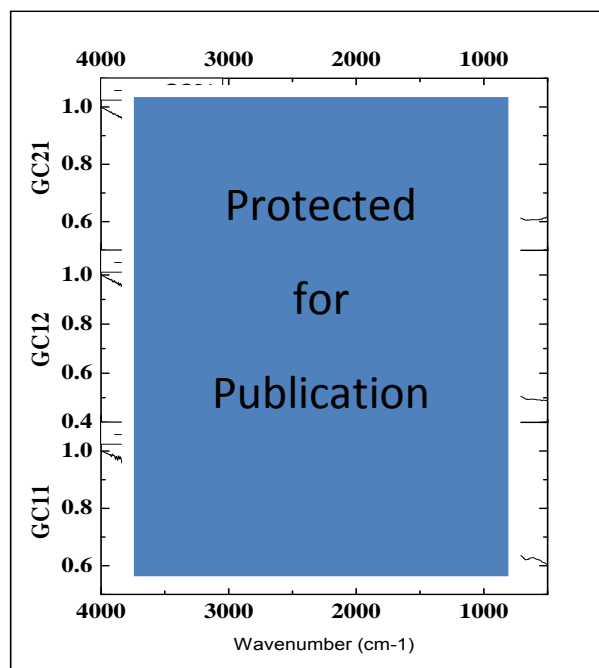


Fig. 7 FTIR spectra of gelatin-chitosan scaffolds

4.2 XRD analysis:

Many papers have reported that gelatin shows a peak at 7° and a broad amorphous peak at around 21° . Chitosan is characterized by two crystalline peaks at $2\theta = 14^\circ$ and 20° . From the X-ray diffractogram, we can observe that in gelatin-chitosan composite scaffold, the crystalline peak of chitosan at $2\theta = 14^\circ$ is no more seen and the crystalline peak at $2\theta = 20^\circ$ seems to get merged with broad amorphous peak of gelatin. A small crystalline peak is obtained at $2\theta = 31^\circ$ in all the three compositions. All the three compositions have similar XRD spectra. Hence, we can

state that varying the composition of gelatin & chitosan has no effect on the atomic structure of composite amorphous scaffold.

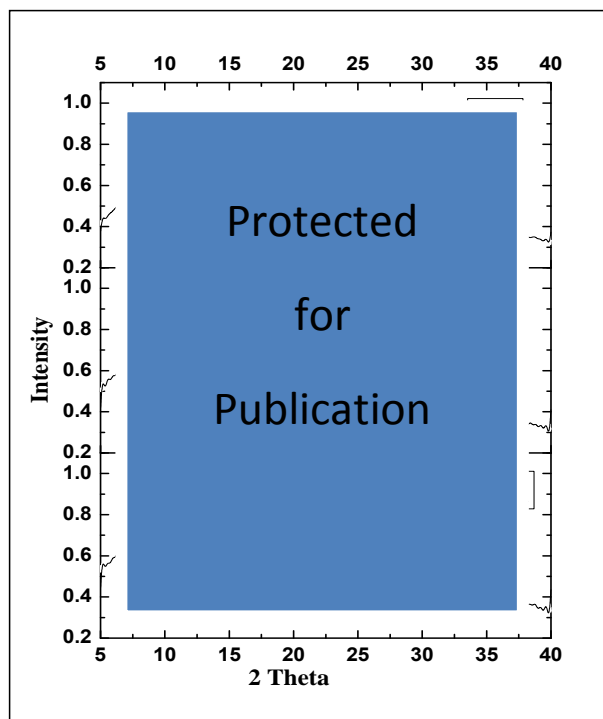


Fig. 8 XRD pattern of gelatin-chitosan scaffolds

4.3 Microstructure analysis:

Surface morphology of gelatin-chitosan scaffold was investigated using scanning electron microscopy to identify any changes in basic microarchitecture due to the variation in gelatin – chitosan composition. It was found that all three types of scaffold have porous structure with apparent interconnectivity. The average pore diameter of GC 21 was found $160 \pm 17 \mu\text{m}$. Same for GC 11 and GC 12 were found $118 \pm 21\mu\text{m}$ and $102 \pm 09\mu\text{m}$ respectively. The average pore diameter seems to decrease with the increase chitosan content. Cell culture on 3D matrix is concerned with the pore size and interconnectivity among the pores in the scaffold is one of the key factors because it greatly influence the nutrient transport process. Moreover, it is observed that cells has some prerequisite of pore diameters which depends on the nature of the cells for successful growth in vitro 3D environment. From that point of view GC 21 seems to be the promising one for three dimensional cell culture.



Fig. 9 Scanning electron micrograph of gelatin-chitosan scaffolds. [A] GC 21 [B] GC 11 [C] GC 12

4.4 Swelling Study:

Among all three scaffolds GC 21 showed highest water retaining capacity. The ability of the scaffold to swell plays an important role during the in-vitro culture studies. Swelling enhances the pore diameter thus helps increasing surface area to volume ratio inside the scaffold which facilitates three dimensional cell attachment and growth. High swelling also ensures maximum availability of nutrients inside the scaffold.

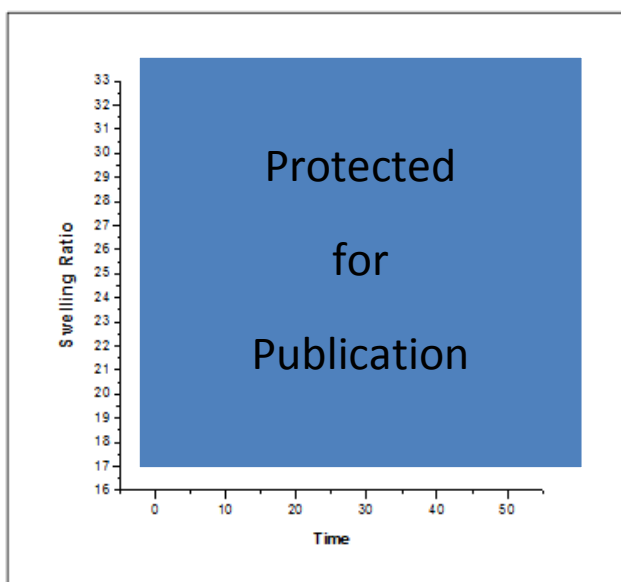


Fig. 10 Swelling kinetics of gelatin-chitosan scaffolds. Values are mean \pm S.D. (n=3)

4.5 Biodegradation Kinetics:

All gelatin-chitosan scaffold degraded in the lysozyme containing PBS as evident from their weight loss which counts up to 45% of the initial dry weight. Biodegradation of gelatin- chitosan

scaffolds are mainly due to the dissolution of gelatin in PBS which is further augmented by lysozyme mediated degradation of chitosan. Though GC 21 showed highest degradation with in 24 hrs (21.73%) but its overall degradation (38.9%) was less compared to other compositions after 7 days.

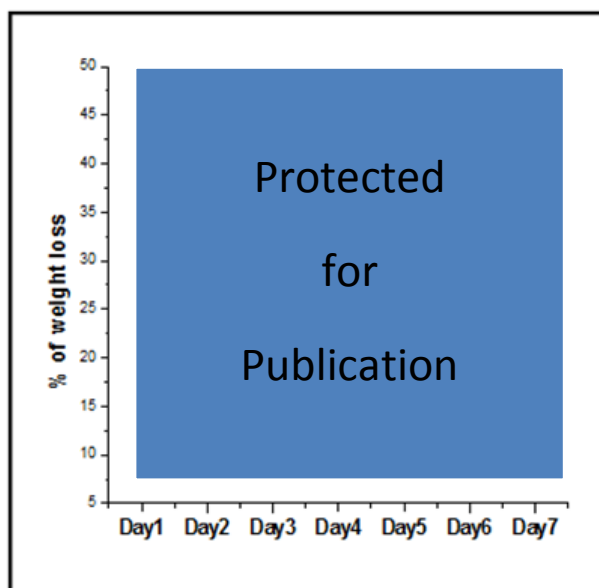


Fig. 11 Biodegradation kinetics of gelatin-chitosan scaffolds. Values are mean \pm S.D. (n=3)

4.6 Biocompatibility:

Highest cell proliferation was observed in case GC 21 in comparison to other compositions and 2D control system as measured by MTT assays. GC 21 scaffold is found to be non-toxic and cytocompatible to HaCaT cells. Healthy conditions of the cells cultured on the scaffold were further confirmed by analyzing SEM micrograph of cell seeded scaffold. Micrograph revealed that cells were three dimensionally organized inside the scaffold.

Experimental results revealed that scaffold with high gelatin content (GC 21) is more reliable than GC 11 and GC 21 as it possesses higher pore size, high water uptake capability and controlled biodegradation. GC 21 was also found to be compatible with HaCaT cells. Considering the physical and functional properties, GC 21 was chosen as a model scaffold for in vitro cell based analysis.

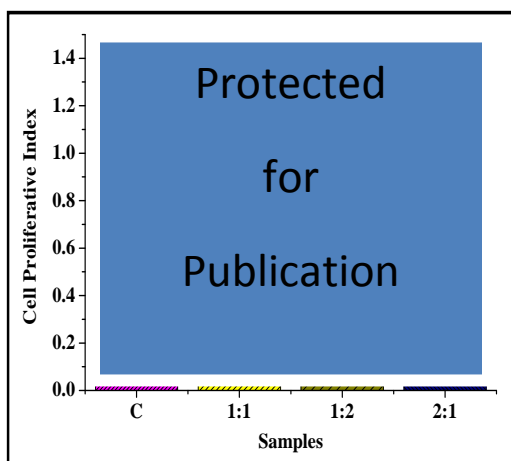


Fig. 12 Biocompatibility of gelatin-chitosan scaffolds with HaCaT cells

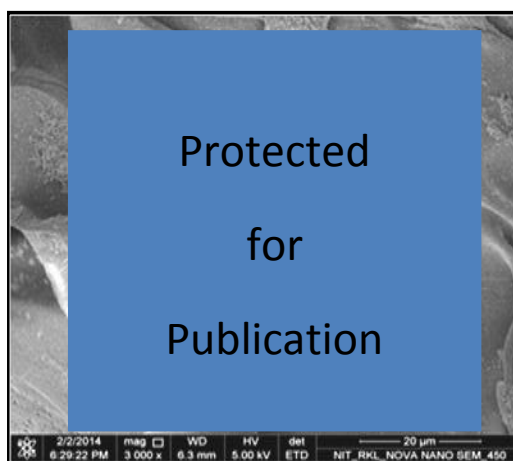


Fig. 13 SEM micrograph of HaCaT cells seeded on GC 21 scaffold

4.7 Scanning Electron Micrograph of HeLa cells in 2D and 3D:

Distribution of cells within the scaffold was visualized by SEM. We already know that cells cultivated directly on tissue culture plates considerably differ in their morphology, cell-cell, cell-matrix interactions from those cells growing in 3D microenvironment. 3D presentation of adhesive ligands by biomaterials influences spindle orientation. HeLa cells on 2D showed flat and elongated morphology.



Fig. 14 Scanning Electron Micrograph of HeLa cells in 2D

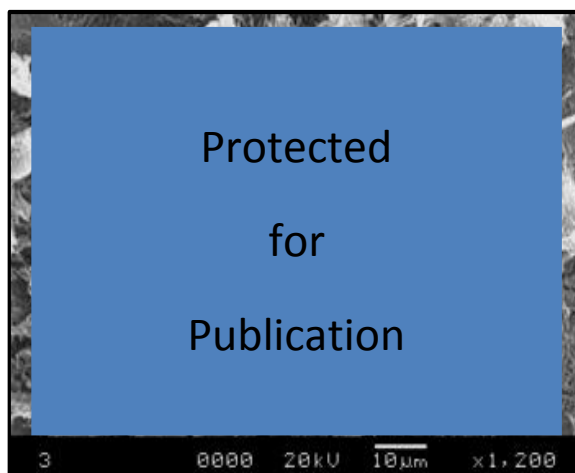


Fig. 15 Scanning Electron Micrograph of HeLa cells seeded on GC 21 scaffold

4.8 Drug sensitivity:

Comparison of 3D and 2D results revealed that, for the same cell seeding density and drug regimen, percentage cell death is more in case of 2D model compared to cell seeded scaffold construct. A significant dose dependent response was obtained after 24 h exposure to 5FU and Cisplatin. HeLa cell seeded scaffolds were more resistant to 5FU and Cisplatin treatment, suggesting poor drug diffusion through the scaffold and lack of complete bioavailability of drug to target cancer cells. Cytotoxicity profile and difference in drug susceptibility between 2D and 3D model is higher in case of cisplatin compared to 5FU which proves that Cisplatin is a more effective & potential drug candidate.

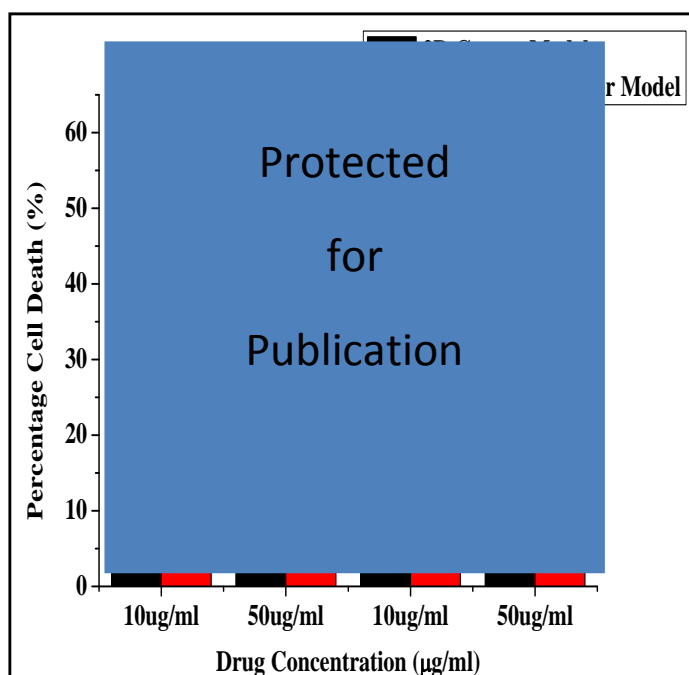


Fig. 16 Percentage cell death in response to varying doses of 5-Fluorouracil and Cisplatin

Chapter 5

FABRICATION OF 3D CANCER MODEL AND EVALUATION OF LAB-ON-A-CHIP DEVICE

5.1 Hanging Drop Technique

Hanging drop technique uses cell suspension droplets hanging from the underside of the lid of tissue culture dish. It utilizes gravity enforced aggregation of cells into a single cluster, which then forms into a spheroid [13]. Due to hydrophilicity of the plate and surface tension of the cell suspension droplet, the drop would hang from the bottom surface of the plate, thereby forming a meniscus in the centre region of the drop. Hanging drop technique is a simple, cost-effective method that allows formation of uniform spheroids of defined size. However, maintaining spheroids in hanging drops requires regular change of medium which is time consuming and inconvenient. Major drawback to using spheroids for large-scale screening is the cumbersome transfer step.

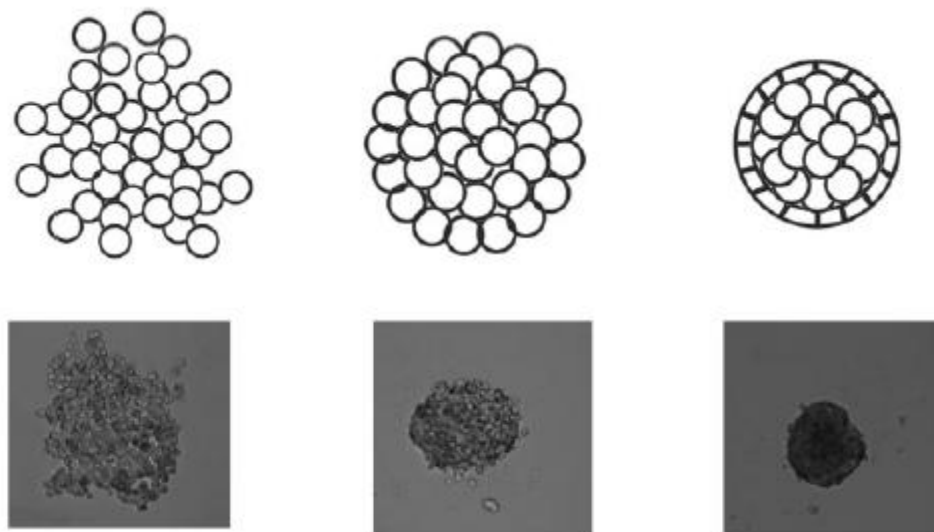


Fig. 17 Cell Aggregation

Compaction

Microtissue Formation

5.2 Microtissue formation

Hanging Drop method was used for making HeLa microtissues. HeLa cells were grown via the hanging drop method over a 6 day experimental period. 25 μL of cell suspension of required cell density was pipetted into a petri dish. Then the tissue culture plate was turned upside down and incubated at 37°C, 5% CO_2 . Gravity driven self assembly of cells results in the formation of microtissue in the centre of the drop. Microtissues were successfully produced in a reproducible manner following this method.

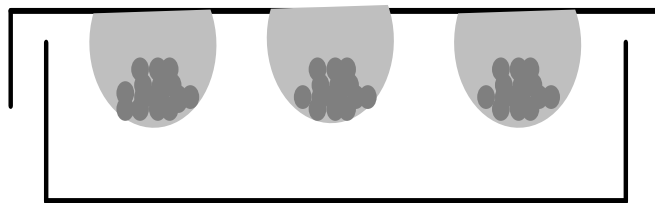


Fig. 18 Hanging Drop Culture

5.3 Microtissue Monitoring and optimization of Cell number

Optimal number of cells required for the formation of microtissue of desired size and compactness was determined by varying cell seeding density, from 10^3 cells to 10^6 cells. Microtissue integrity was visualized by phase contrast microscope, which can also be used for recording microtissue volume growth kinetics. Images for quantitative analysis of the size distribution and shape of HeLa microtissue were routinely captured by phase contrast microscopy at day 4, day 5 & day 6 after seeding. Compactness profile and size kinetics of microtissue from day 4 to day 6 was plotted using ImageJ.

5.4 Seeding Microtissue on the scaffold:

Scaffolds were neutralized and sterilized using the protocol mentioned in 3.5.6 (i). Microtissue transfer was achieved by direct pipetting using a tip whose top portion has been removed so as not to disrupt the microtissue by shear or stress. Individual microtissues were retrieved from the petri dish and then gently pipetted into fresh culture dish (35mm dia). Three intact HeLA microtissues were seeded on each scaffold. The seeded constructs were incubated in a humidified CO_2 incubator for 2 days to allow microtissue growth and proliferation within the 3D microenvironment of the porous scaffold. Viability of microtissue seeded scaffold constructs was accessed by MTT assay. The control system included (i) HeLa cells directly cultured in the microwell at the same cell density as present in the microtissue (ii) HeLa microtissue directly cultured in the microwell (iii) HeLa cells directly seeded on the scaffold at the same cell density as present in the microtissue. Cell proliferation in each case was plotted using 2D monolayer system as reference and comparative analysis was performed.

5.5 Drug Susceptibility:

To validate the 3D cancer model, it is necessary to screen its chemotherapeutic susceptibility to anticancer drugs. Microtissues were seeded on the scaffold and their chemotherapeutic sensitivity was evaluated using 5-FU and Cisplatin at a concentration of 50ug/ml for each drug. Effect of these cytotoxic agents on cell viability within the microtissue present in the 3D microenvironment of scaffold was accessed by MTT assay using previously described control systems. Percentage cell death recorded with two drugs was plotted and comparative analysis was performed.

5.6. Cryopreservation:

The word Cryopreservation is composed of two words "cryo" and "preservation". "Cryo" meaning cells or tissue and "preservation" meaning to the act of preserving something. It is a process in which cells or any other substances which might be damaged due course of time or due to chemical reactivity are preserved by cooling to ultra low temperatures. At very low temperatures, the possibility of damage due to enzymatic or chemical activity is effectively stopped. This is attained without causing additional damage due to the formation of ice crystals during freezing. Advantages of cryopreservation are listed as follows:

- Lowered risk of contamination by microorganisms
- Lowered risk of cross contamination of cells by other cell lines
- Lowered risk of morphological and genetic changes
- Cost effective

Temperature: Sub-zero temperatures provide indefinite longevity to the cells. However, it is difficult to predict the actual effective life. Boiling point of liquid nitrogen (-196°C or 77 K or -321°F), the, is the preferred temperature for cryogenic storage. When adequate cryogenic facilities are unavailable, refrigerators and extra-cold freezers are often used for cooling. Generally ultra-cold liquid nitrogen is required for successful cryopreservation in order to virtually stop all biological and enzymatic activity.

Cryoprotective agents: Cryoprotective agents have the ability to enter cells and to prevent dehydration and formation of ice crystals in the cytoplasm of the cells, which can cause destruction of cell organelles and cell death. Two common cryoprotective agents are dimethyl sulfoxide (DMSO) and glycerol. Glycerol is used for cryoprotection of RBC's, and DMSO is most commonly used for protection of other cells and tissues.

5.6.1 Cryopreservation of Microtissue seeded scaffold construct:

Evaluation of anticancer drug efficacy in *in-vitro* 3D cancer model necessitates careful investigation of its cryopreservation performance. Cryopreservable 3D cancer model plays a very important role in terms of its “ready-to-use” application in drug screening after resuscitation. We investigated whether microtissue seeded scaffold construct could be cryopreserved for “ready-to-use” applications. The cryopreservable and tumorigenic 3-D cancer model offers an effective platform for drug screening. Lot of research work has been undertaken to ensure successful cryopreservation and resuscitation of cancer models. Successful cryopreservation is based on the basic principle of a slow freeze and thaw cycle. Although the requirements of different cells would vary, the general guidelines are: cells must be cooled at a rate of -1°C to -3°C per minute and quickly thawed by incubating the cryovials in a 37°C water bath for 3-5 minutes. If this is followed then most cells should be cryopreserved successfully.

5.6.2 Cryopreservation Protocol

i) Preparation of Cryopreservation medium:

Cryopreservation medium should have the same formulation as that used to cultivate cells with the addition of FBS in case of serum-free cultures or with the increase in the concentration of FBS, but to a final concentration of not more than 20%. FBS performs the role of binding toxic materials which may be released if some cells are lysed during the freezing or thawing process. Using a cryopreservative agent is a must requirement. Either of the two - DMSO or glycerol can be used, primary choice being sterile DMSO. The following composition of cryopreservation medium was standardized for use in all our experiments:

Dimethyl Sulphoxide (DMSO)	10%
Culture Media (MEM)	20%
Fetal Bovine Serum (FBS)	80%

ii) Freezing:

Microtissue seeded scaffold was immersed in cryovials, each containing 2 ml cryopreservation medium. Vials were first placed in 4°C freezer for 30 minutes and then in -20°C for 2 h and subsequently in -80°C freezer for 4 h. The vials will freeze slowly after which they were directly transferred to liquid nitrogen storage tank.

iii) Thawing cryopreserved system:

After 24 h, microtissue seeded scaffold system was resuscitated/ retrieved quickly to obtain the best possible viability. Once the cryovial was removed from liquid nitrogen tank, it was directly submersing in pre-warmed distilled water at 37°C for 1-2 minutes. Cell viability was assessed by MTT assay. Control system used is microtissue seeded scaffold cultivated in a humidified incubator (37°C, 5% CO₂) for 48 h.

Key points:

- Cryopreservation medium must be prepared fresh each time.
- Cryoprotective agents must always be used at an appropriate concentration so as to avoid viability issues.
- Cryoprotective agents tend to rapidly oxidize or absorb potentially toxic materials from the air. Hence, they must be used fresh each time. Large volumes should not be procured. Reagent bottle must not be continuously opened and closed.
- Personal protective equipments must be wore at all times while handling cryovials from liquid nitrogen tank. Liquid nitrogen will expand drastically around 700 times during the warming process. Hence, care must be taken while removing cryovials from liq N₂ storage tank as there can be chance of explosion, if liquid nitrogen has entered the cryovial. Cryovials once removed from liquid nitrogen tank must be quickly transferred to 37°C water bath.

Chapter 6

RESULTS AND DISCUSSION

6.1. Optimization of Cell number:

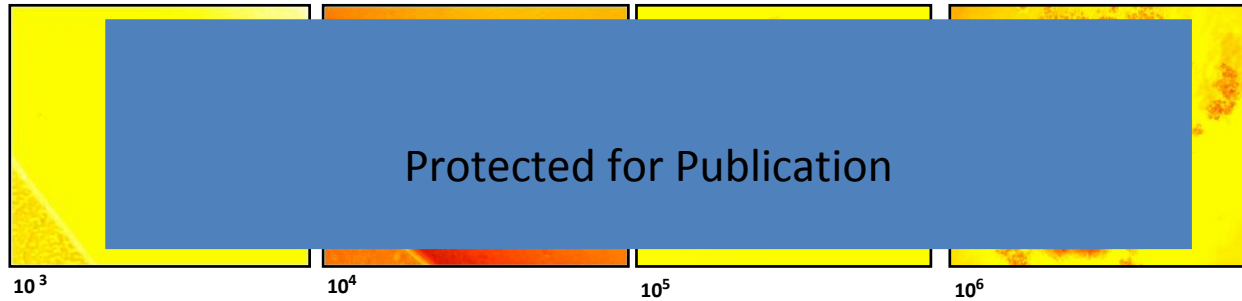


Fig.19 Phase contrast images of Microtissue at different cell density per drop

The process of embryonic development is thermodynamically regulated during which specific number of cells are involved in complex cell-cell adhesion thereby forming morula. A similar mechanism is observed in microtissue formation. Microtissue size can be fine-tuned by changing the seeding density of cells. With lesser number of cells (10^3 and 10^4), microtissue formed is loosely bound and not compact. Increasing the cell density to 10^5 cells per drop, yielded a compact microtissue with a central dense core. However with 10^6 cells, a loosely bound microtissue was obtained. Hence, we could conclude that 10^5 cells is the optimal cell density required for the formation of a uniform pool of compact microtissues. 10^5 HeLa cells spontaneously aggregate into viable 3D microtissue or microscale spheroids when cultured in environments where cell-cell interactions dominate over cell-substrate interactions.

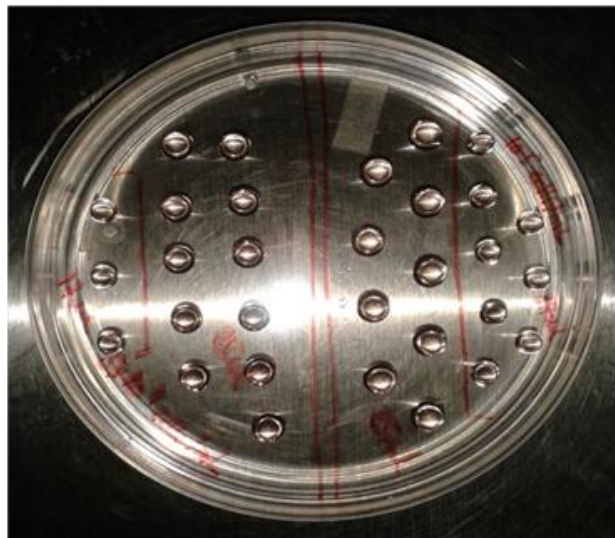


Fig.20 Approximately 32 hanging drops deposited and grown under a 15-cm dish lid

6.2 Microtissue Compactness and Area growth kinetics:

Spheroid morphology was routinely monitored from day 4 to day 6. It was observed that microtissue diameter continued to increase until day 6 with the loss of tight packing between the cells. Surface plots were drawn using ImageJ to visualize the compactness of microtissue. On day 4, cells were tightly bound to each other, and individual cells were no more observed. With increase in time, the aggregates became less denser and its diameter kept increasing. Longer culturing time (>5 days) lead to a significant loss of compactness and increase in the microtissue diameter. Size of the microtissue increased as a function of time. 4 days of culture produced uniformly sized HeLa microtissues with an average size of 2mm, at the initial seeding density of 10^5 cells/mL.

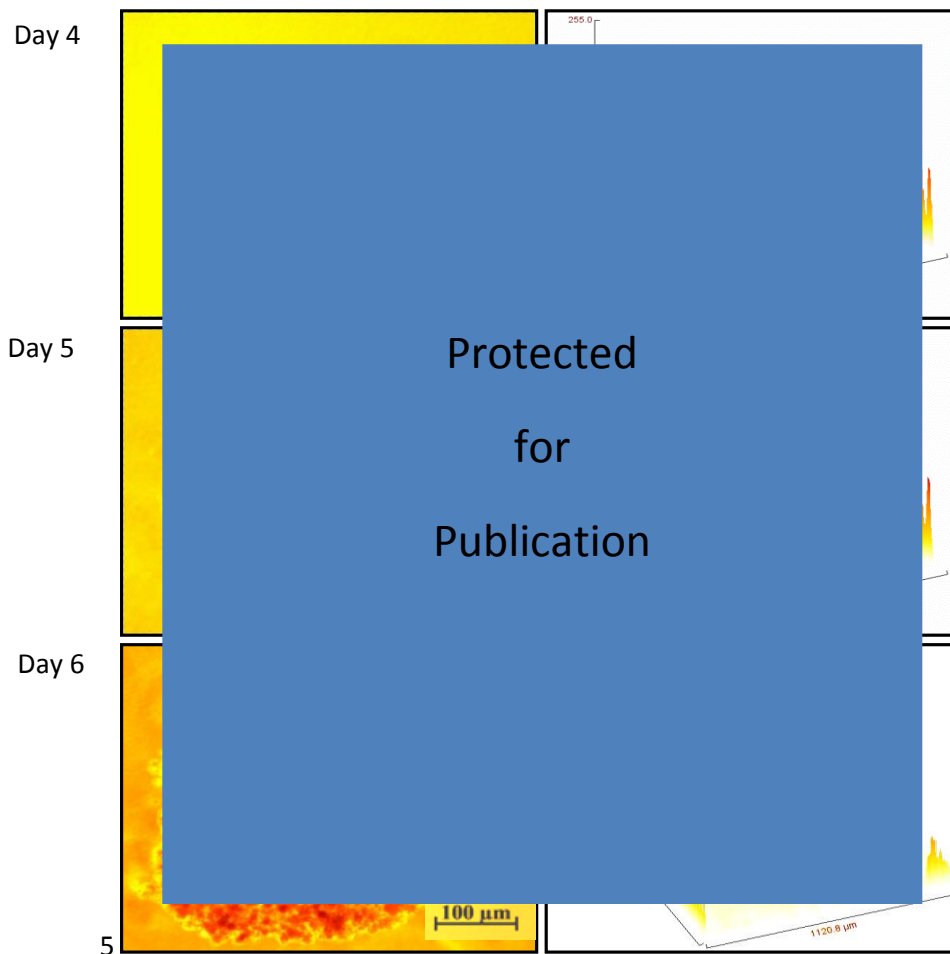


Fig. 21 Phase Contrast Images and Compactness profile of microtissue at day 4, 5 and 6

Area growth kinetics revealed the exponential increase in the area of microtissue over a 7 day experimental period. Optimal microtissue formed after 4 days of culture. Hence, aggregated HeLa microtissues were obtained from 10^5 cells after 4 days of culture.

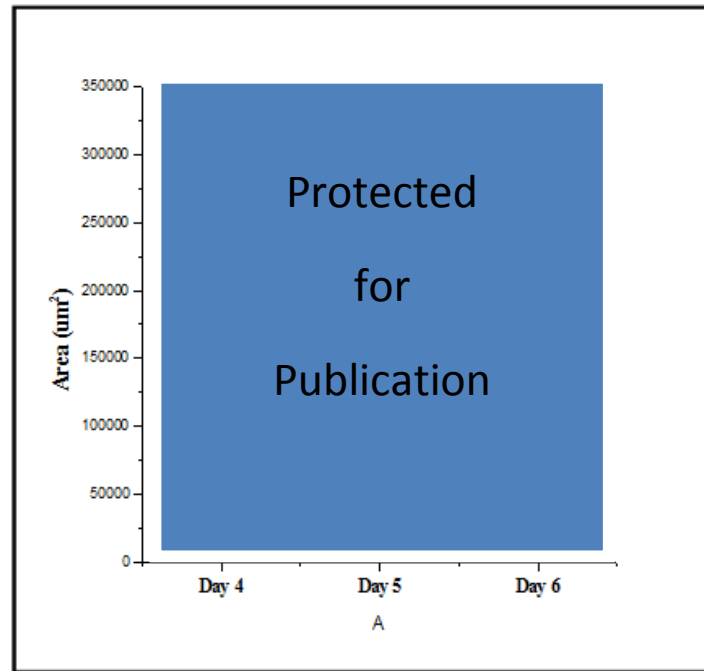


Fig. 22 Area growth profile of microtissue from day 4 to day 6

6.3. Viability Assay of Microtissue seeded scaffold

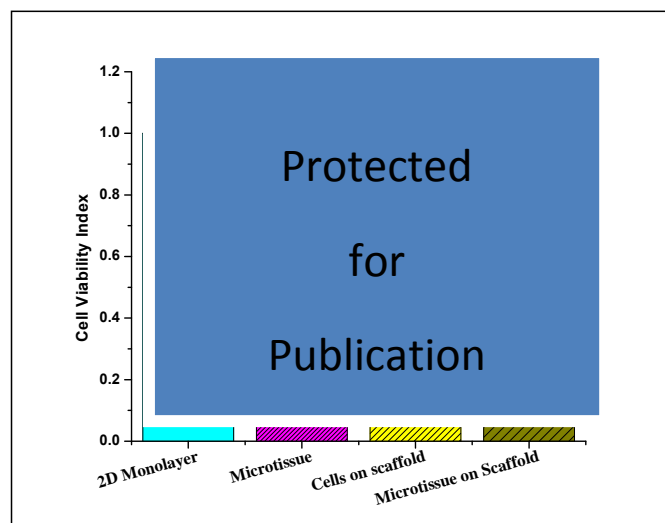


Fig. 23 Cell proliferation index of microtissue seeded scaffold construct compared to control system

Simply, HeLa cell seeded scaffold does not recapitulate the intimate cell-cell architecture found in normal tissue. Rather, it closely approximates a culture system in which single cells are loosely dispersed within a 3D ECM meshwork. 3D microtissue seeded scaffold model showed higher viability compared to control counterparts. This is due to an intricate network of cell-cell interactions under the influence of native ECM like scaffold. Porous nature of the scaffold mimicking native ECM provides 3D microenvironment to the in-vivo like tumor masses, the microtissues which progressively grow and hence show higher viability.

6.4 Anticancer drug cytotoxicity study:

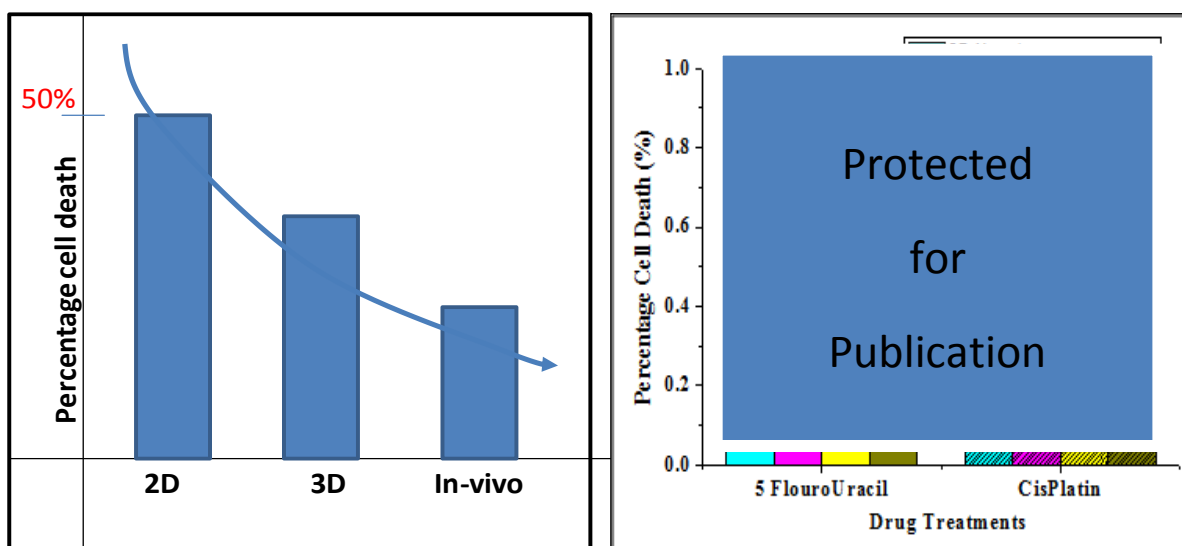


Fig. 24 Percentage cell death of microtissue seeded scaffold construct compared to control system and theoretical predictions.

Cytotoxicity of 5FU and Cisplatin was evaluated in in-vitro 3D tumor model with microtissue encapsulated in the scaffold and compared to control system. Chemotherapeutic sensitivity of the cancer cells varies with microenvironment especially when moving from 2D monolayer to 3D solid tumor like environment. Comparison of 2D and 3D results revealed that upon treatment with 5-FU and Cisplatin, percentage cell death in 3D model was approximately 58% and 62% respectively in comparison to approximately 76% and 80% respectively in 2D. 3D microtissues were more chemoresistant than 2D monolayer due to the presence of quiescent cells in microtissue. This resistance to therapeutics in case of 3D model is thought to be associated with

the three dimensional organizations of cells within the matrix and poor diffusion of drug molecules through the microtissue and scaffold. Because the proposed 3D tumor model bears close resemblance to in-vivo human cancer tissues both morphologically and physiologically, the toxicity derived from this is more accurate than the false positive cytotoxicity results obtained in 2D monolayer cells.

6.5 Cryopreservation performance:

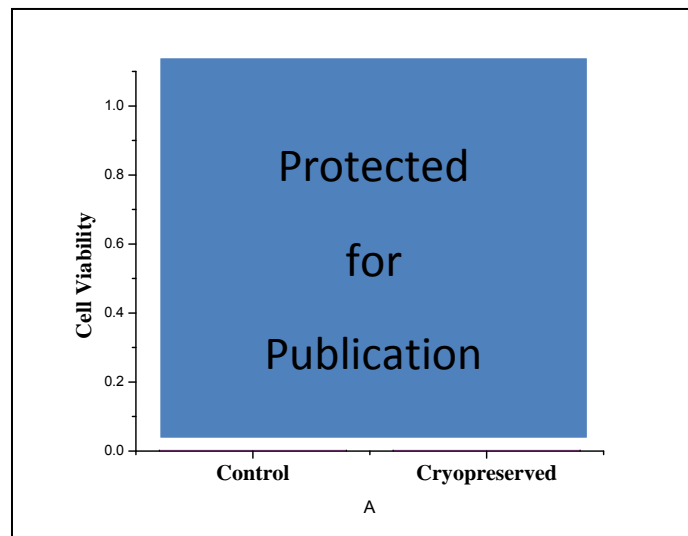


Fig. 25 MTT Assay of cryopreserved microtissue seeded scaffold construct compared to control system which was not cryopreserved

Compared to control system which was not cryopreserved, 76% cell viability was attained after resuscitating cryopreserved 3D model. This is significant and implies that long term storage of our system is feasible for ready to use drug screening applications. Viability can further be increased by carefully monitoring the process of controlled rate freezing and thawing.

CONCLUSION

3D cancer models with *in vivo* like characteristics of cell–cell, cell–matrix interactions are powerful tools for drug screening. Proposed 3D cancer model of microtissue encapsulated in gelatin-chitosan scaffold closely mimics in-vivo tumor and acts as a promising screening tool for various existing and novel cancer therapies, including nanoparticles, liposomes, and nonviral gene delivery. Anti-proliferative effect of anticancer drugs in 3D model was significantly lower compared to 2D monolayer. Direct correlation between the results of drug effects observed in our model to the theoretically predicted in-vivo efficacy establishes the usefulness of our model in drug discovery and development. It is physiologically more relevant than 2D systems and animal models. The proposed model offers an economically advantageous in-vitro platform for testing drug delivery systems. The model is convenient to be handled and easy for any lab to maintain or reproducibly manufacture. Its impact lies in the benefits it offers for investigating the chemotherapeutic efficiency of anticancer therapeutics with relatively low costs.

Key Features of the proposed model:

1. Highly controllable and reproducible
2. Relatively low cost
3. High in-vivo like characteristics and predictivity
4. More physiologically relevant than 2D monolayer and spheroid model
5. Cryopreservable
6. Ready-to-use, no mixing and preparation method
7. Easy for any lab to maintain & readily use for screening new drugs

FUTURE WORK

- 1.** Monitoring and understanding the process of tumor vascularization - angiogenesis.
- 2.** Visualizing the surface morphology of microtissue by Scanning Electron Microscopy.
- 3.** Visualizing the internal structure of microtissue by Transmission Electron Microscope.
- 4.** Live/dead assay of HeLa microtissue by flow cytometry
- 5.** Cell cycle analysis of microtissue and cells in monolayer by flow cytometry.
- 6.** Visualizing the penetration behavior of anticancer therapeutics into individual microtissue and distribution of drug in the microtissue seeded scaffold construct.
- 7.** Examining drug uptake kinetics in individual microtissue as a function of time which would allow and determination of effective diffusion coefficients.
- 8.** Prepare microtissues comprising multiple cell types - heterogeneous tumor/stromal cell co-culture (fibroblast cells, immune cells etc.) to mimic in-vivo tumor heterogeneity.
- 9.** Upgrade the sensitivity, and compatibility of developed lab-on-a-chip device with high-throughput screening (HTS) instruments.
- 10.** Optimize cryopreservation to improve viability post resuscitation.
- 11.** Study cellular migration and tumor dissemination within the 3D microtissue seeded scaffold constructs.

REFERENCES

Patents

1. Malathy P.V.Shekhar, "**Three-Dimensional in-vitro Model of Human Preneoplastic Breast disease**," U.S Patent US 6,828, 111 B2, Dec.7, 2004
2. HOFFMAN, Robert M., "**In-vitro model for HIV and other viral diseases**," Patent WO 98/23729, 4 June, 1998.
3. Masahiro Inoue, "**Culture method, evaluation method and storage method for cancer-tissue-derived cell mass or aggregated cancer cell mass**," U.S Patent US 20130012404 A1, Jan 10, 2013
4. Herve Jouishomme, Jenny Phipps, Michel Phipps, Suzanne Lacelle, "**3-dimensional in vitro models of mammalian tissues**," Patent WO 2000075286 A2, Dec 14, 2000
5. Domokos Bartis, Judit Erzsébet PONGRÁCZ, "**Lung tissue model**," Patent WO 2012059777 A1, May 10, 2012
6. Banerjee, Debabrata, "**Reconstituted Tumor Microenvironment for Anticancer drug development**," U.S Patent 20120213706, Aug. 23, 2013. Anant, Shrikant, "**In vitro tumor in dish kit and method**," U.S Patent 20130316392, Nov. 28, 2013

Papers

1. Ajit S.Narang. (2001). **Unique Aspects of Pharmaceutical Development**. In: Bruce C. Baguley and David J. Kerr. *Anticancer Drug Development*. New Jersey: Pharmaceutical Perspectives of Cancer Therapeutics. 49-92.
2. Amy Y. Hsiao. (2012). **384 Hanging Drop Arrays Give Excellent Z-Factors and Allow Versatile Formation of Co-Culture Spheroids**. *Biotechnology and Bioengineering*. xxx (xxx).
3. Giorgia Imparato. (2013). **The role of microsccaffold properties in controlling the collagen assembly in 3D dermis equivalent using modular tissue engineering**. *Biomaterials*. 34 (1), 7851-7861.
4. Crystal S. Shin. (2013). **Development of an in Vitro 3D Tumor Model to Study Therapeutic Efficiency of an Anticancer Drug**. *Mol Pharm.* 10 (6), 2167-75.

5. Hui-li Ma. (2012). **Multicellular Tumor Spheroids as an In Vivo–Like Tumor Model for Three-Dimensional Imaging of Chemotherapeutic and Nano Material Cellular Penetration.** *Molecular Imaging.* 11 (6), 487-498.
6. Qingyi He. (2013). **A tissue-engineered subcutaneous pancreatic cancer model for antitumor drug evaluation.** *International Journal of Nanomedicine.* 8 (1), 1167–1176.
7. Agata Nyga. (2013). **A novel tissue engineered three-dimensional in vitro colorectal cancer model.** *Acta Biomaterialia.* 9 (1), 7917–7926.
8. Jayme L. Horning, Sanjeeb K. Sahoo. (2008). **3-D Tumor Model for In Vitro Evaluation of Anticancer Drugs.** *Molecular Pharmaceutics.* 5 (5), 849–862.
9. Chandraiah Godugu. (2013). **AlgiMatrix™ Based 3D Cell Culture System as an In-Vitro Tumor Model for Anticancer Studies.** *PLOS ONE.* 8 (1), 1-13.
10. Y.Huang. (2005). **In vitro characterization of chitosan–gelatin scaffolds for tissue engineering.** *Biomaterials.* 26 (36), 7616-7627
11. Rati Lama. (2013). **Development, validation and pilot screening of an in vitro multi-cellular three-dimensional cancer spheroid assay for anti-cancer drug testing.** *Bioorganic & Medicinal Chemistry.* 21 (1), 922–931.
12. K.M.Yamada. (2007). **Modeling Tissue Morphogenesis and Cancer in 3D.***Cell.* 130 (4), 601-10
13. R.Hamid. (2004). **Comparison of alamar blue and MTT assays for high through-put screening.** *Toxicol In Vitro.* 18 (5), 703-710
14. M.J.Corral. (2013). **Improvement of 96-well microplate assay for estimation of cell growth and inhibition of Leishmania with Alamar Blue.** *Journal of Microbiological Methods.* 94 (2), 111-116
15. M Mendoza-Aquilar. (2012). **The use of the microplate alamar blue assay (MABA) to assess the susceptibility of Mycobacterium lepraemurium to anti-leprosy and other drugs.** *J Infect Chemother.* 18 (5), 652-61
16. S Al-Nasiry. (2007). **The use of Alamar Blue assay for quantitative analysis of viability, migration and invasion of choriocarcinoma cells.** *Hum Reproduc..* 22 (5), 1304-9
17. RC Borra. (2009). **A simple method to measure cell viability in proliferation and cytotoxicity assays.** *Braz Oral Res..* 23 (3), 255-62

18. J O'Brien. (2000). **Investigation of the Alamar Blue (resazurin) fluorescent dye for the assessment of mammalian cell cytotoxicity.** *Eur J Biochem.* 267 (17), 5421-6
19. AY Hsiao. (2012). **384 Hanging Drop Arrays Give Excellent Z-factors and Allow Versatile Formation of Co-culture Spheroids.** *Biotechnol Bioeng.* 109 (5), 1293-304
20. KC.Kavya. (2013). **Fabrication and characterization of chitosan/gelatin/nSiO₂ composite scaffold for bone tissue engineering.** *Int J Biol Macromol.* 59 (1), 255-63
21. E.Jeevithan. (2013). **Physico-functional and mechanical properties of chitosan and calcium salts incorporated fish gelatin scaffolds.** *International Journal of Biological Macromolecules.* 60 (1), 262-267
22. M.Alizadeh (2013). **Microstructure and characteristic properties of gelatin/chitosan scaffold prepared by a combined freeze-drying/leaching method.** *Mater Sci Eng C Mater Biol Appl.* 33 (7), 3958-67
23. H Jiankang. (2009). **Preparation of chitosan-gelatin hybrid scaffolds with well-organized microstructures for hepatic tissue engineering.** *Acta Biomater.* 5 (1), 453-61
24. Khairul Anuar Mat Amin. (2011). **Polyelectrolyte complex materials from chitosan and gellan gum.** *Carbohydrate Polymers.* 86 (1), 352-358
25. Anand S. Deshmukh. (2012). **Gum ghatti: A promising polysaccharide for pharmaceutical applications.** *Carbohydrate Polymers.* 87 (2), 980-986
26. L. Liu. (2013). **Chitosan fibers enhanced gellan gum hydrogels with superior mechanical properties and water-holding capacity.** *Carbohydr Polym.* 97 (1), 152-8
27. JB.Kim. (2005). **Three-dimensional tissue culture models in cancer biology.** *Semin Cancer Biol.* 15 (5), 365-77
28. YS.Torisawa. (2005). **Multi-channel 3-D cell culture device integrated on a silicon chip for anticancer drug sensitivity test.** *Biomaterials.* 26 (14), 2165-72
29. V. Tandon. (2013). **Generation of tissue constructs for cardiovascular regenerative medicine: From cell procurement to scaffold design.** *Biotechnol Adv.* 31 (5), 722-35
30. BB Mandal. (2008). **Non-Bioengineered Silk Fibroin Protein 3D Scaffolds for Potential Biotechnological and Tissue Engineering Applications.** *Macromol Biosci.* 8 (9), 807-18
31. Zorlutuna P. (2013). **The Expanding World of Tissue Engineering: The Building Blocks and New Applications of Tissue Engineered Constructs.** *IEEE Rev Biomed Eng.* 6 (1), 47-62

32. Kunz-Schughart LA. (2004). **The Use of 3-D Cultures for High-Throughput Screening: The Multicellular Spheroid Model.** *J Biomol Screen.* 9 (4), 273-85
33. R.Wang. (2005). **Three-dimensional co-culture models to study prostate cancer growth, progression, and metastasis to bone.** *Semin Cancer Biol.* 15 (5), 353-64
34. Moutushy Mitra. (2012). **A novel in vitro three-dimensional retinoblastoma model for evaluating chemotherapeutic drugs.** *Molecular Vision.* 18 (1), 1361-1378.
35. Guojie Xu. (2014). **In vitro ovarian cancer model based on three-dimensional agarose hydrogel.** *Journal of Tissue Engineering.* 5 (1), 576-590.
36. Jong Bin Kim. (2004). **Three-dimensional in vitro tissue culture models of breast cancer – a review.** *Breast Cancer Research and Treatment.* 85 (1), 281–291
37. Sun-Woong Kang, You Han Bae. (2009). **Cryopreservable and Tumorigenic Three Dimensional Tumor Culture in Porous Poly(lactic-co-glycolic acid) Microsphere.** *Biomaterials.* 25 (2), 4227-32.